Looking for a light Higgs boson in the Zγ→ll[over ¯]γ channel

James S. Gainer, Wai-Yee Keung, Ian Low, and Pedro Schwaller

Phys. Rev. D **86**, 033010 — Published 24 August 2012

DOI: 10.1103/PhysRevD.86.033010

Looking for a light Higgs boson in the $Z\gamma$ channel

James S. Gainer[a,b], Wai-Yee Keung[c], Ian Low[a,b], and Pedro Schwaller[a,c]

[a] *High Energy Physics Division, Argonne National Laboratory, Argonne, IL 60439*
[b] *Department of Physics and Astronomy, Northwestern University, Evanston, IL 60208*
[c] *Department of Physics, University of Illinois at Chicago, IL 60607*

The final state obtained when a Higgs boson decays to a photon and a Z boson has been mostly overlooked in current searches for a light Higgs boson. However, when the Z boson decays leptonically, all final state particles in this channel can be measured, allowing for accurate reconstructions of the Higgs mass and angular correlations. We determine the sensitivity of the Large Hadron Collider (LHC) running at center of masses energies of 8 and 14 TeV to Standard Model (SM) Higgs bosons with masses in the $120 - 130$ GeV range. For the 8 TeV LHC, sensitivity to several times the the SM cross section times branching ratio may be obtained with 20 inverse femtobarns of integrated luminosity, while for the 14 TeV LHC, the SM rate is probed with about 100 inverse femtobarns of integrated luminosity.

Introduction – The search for the Higgs boson is entering a critical phase. Data collected at the LHC rules out the SM Higgs boson for a wide range of masses and may suggest a Higgs boson with mass near 125 GeV [1, 2]. Searches for a light SM Higgs in the still-relevant mass window rely primarily on the $\gamma\gamma$ decay channel, though the $WW^* \to 2\ell 2\nu$ decay channel and the "golden" $ZZ^* \to 4\ell$ decay channel are also important (here V^* indicates an off-shell gauge boson).

So far very little attention has been given to the $Z\gamma \to \ell\bar{\ell}\gamma$ channel [3], although its event rate is comparable to that of the golden channel for a light SM Higgs boson. The rates for these processes are similar because while the branching fraction for Higgs to $Z\gamma$ (about 1.5×10^{-3} for a 125 GeV Higgs [4]), is lower than that for Higgs to ZZ, only one Z must decay to leptons rather than two, and the branching fraction for $Z \to l\bar{l}$ is relatively small.

Despite the relative lack of attention, the $Z\gamma$ decay channel has the advantage that all final state particles can be measured well, which carries several important implications: 1) the Higgs mass could be measured from the total invariant mass spectrum, 2) the spin of a putative signal can be determined by studying angular correlations [5], and 3) the separation of signal from background can be facilitated by employing full kinematic information, potentially allowing searches with enhanced sensitivities. For the golden channel in $ZZ^* \to 4\ell$ the above questions have been studied extensively [6–8], but we are not aware of any detailed studies for the $Z\gamma$ channel.

Measurements of all four Higgs decay modes into electroweak bosons are in fact very important in determining the electroweak quantum numbers of a putative Higgs signal [9]. Furthermore, an electroweak singlet scalar could easily have a branching fraction in the $Z\gamma$ mode that is orders of magnitude larger than the SM expectation [10] which provides an important additional incentive for studying this channel.

In this work we investigate the sensitivity of the 8 and 14 TeV LHC to the SM Higgs boson in the $h \to Z\gamma \to l\bar{l}\gamma$ decay channel. We use cut-based analyses which employ a discriminant function. We compare the sensitivity obtained when this discriminant function is multivariate (essentially the leading order differential cross section) to the sensitivity obtained when this discriminant uses only invariant mass information and find that they are similar. We therefore quote results from obtained using the invariant-mass based discriminant, as these should be more robust to systematic effects. In the next section we describe the kinematic features of the signal and background processes, which motivate the consideration of a multivariate discriminant. This is followed by a more detailed description of our analysis procedure and the results we obtained.

Kinematics: Definition of Angles – The kinematics of the final state in $Z\gamma \to \ell\bar{\ell}\gamma$ events is described by three angles, Θ, θ and ϕ, where Θ may be taken to be the angle describing the production of the Z boson in the center of mass frame, and θ and ϕ are the angles that describe the decay of the Z to leptons.

More specifically the angles are defined as followed:

1. We define the lab frame such that the three momentum of the $Z\gamma$ system is in the positive $\hat{z}$ direction.

2. We then boost along the z axis to the rest frame of the $Z\gamma$ system.

3. Then we define the x-axis in this frame so that the Z boson three momentum is in the xz-plane with positive momentum in the x-direction.

4. We define Θ as the angle of the Z three momentum with respect to the positive z-axis in this frame.

5. Next, we rotate about the y-axis by this angle Θ so that the Z boson three momentum is in the z-direction.

6. We then boost along this z-axis to the rest frame of the Z. In this frame, the three momentum of the lepton is given by $|\mathbf{p}_\ell|(\sin\theta\cos\phi, \sin\theta\sin\phi, \cos\theta)$. This defines θ and ϕ.

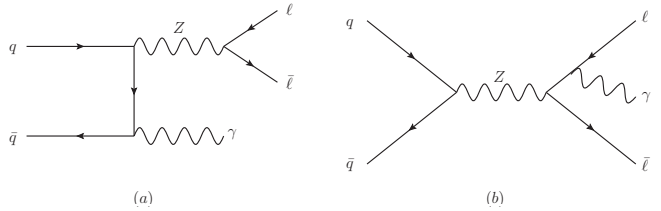

FIG. 1: *Feynman diagrams contributing to $q\bar{q} \to \ell\bar{\ell}\gamma$ are shown in (a) and (b).*

Lorentz invariant expressions in the analogous $ZZ \to 4\ell$ case are given, for the case of no additional jet radiation, in [8].

Kinematics: Properties of Signal and Background –

The dominant irreducible background to the Higgs signal arises from initial state radiation (ISR) and final state radiation (FSR) from Drell-Yan production of a Z boson; diagrams describing these processes are shown in Fig. 1 (a) and (b). The invariant mass of the $Z\gamma$ system from FSR events is close to the Z boson mass, so this background is removed efficiently by imposing $m_{\ell\ell\gamma} > 100$ GeV, thus we can focus on the ISR background (as represented by diagram (a)) and the corresponding u-channel diagram for the rest of this analysis.

We will not consider the main reducible background, which consists of events where the Drell-Yan production of a Z boson is accompanied by a jet that is reconstructed as a photon. Such events constitute perhaps $20 - 30\%$ of the sample of nominally $Z\gamma$ events which one obtains after preselection cuts [11, 12]. Thus one should expect some degradation of sensitivity compared with the results we will quote. Determining this effect precisely is challenging as it involves the specifics both of the detector and of the definitions for photon and jet objects chosen for the analysis, which can be tuned to optimize signal sensitivity. Hence we leave the treatment of this issue for more detailed experimental studies.

The signal and irreducible background cross sections were computed using the helicity basis in [13]. We now discuss some qualitative features of these differential cross sections, in particular the Θ dependence of the signal and background processes.

In the signal case, angular distributions follow from the fact that the Higgs is a scalar particle, and hence only the decay angle θ has a nontrivial distribution:

$$\frac{d\sigma}{d\cos\Theta\, d\cos\theta\, d\phi} \propto (1 + \cos^2\theta) \ , \tag{1}$$

The insensitivity to other decay angles is due to the fact that $Z\gamma$ can only have the helicity combinations $(\lambda_1, \lambda_2) = (\pm 1, \pm 1)$, where λ_1 is the helicity of the Z boson, and λ_2 is the helicity of the photon.

For the background distributions, all helicity combinations are non-vanishing. The production angular distribution exhibits a collinear singularity at $\cos\Theta = \pm 1$, which is seen by examining the t-channel propagator in Fig. 1 (a),

$$\frac{1}{(k_{\bar{q}} - p_\gamma)^2} = -\frac{1}{2E_{\bar{q}}E_\gamma(1 - \cos\Theta)} \ , \tag{2}$$

while the u-channel propagator gives the collinear singularity at $\cos\Theta = -1$. Thus the production angular distribution for the background process is peaked at $\cos\Theta = \pm 1$, producing forward and backward photons. The singularity is removed by the p_T cuts on the photon and leptons. Explicit (leading order) calculations lead to

$$\frac{d\sigma}{d\cos\Theta\, d\cos\theta\, d\phi} \propto (g_r^2 + g_\ell^2)(g_R^2 + g_L^2)\,\mathcal{G}_1 + (g_r^2 - g_\ell^2)(g_R^2 - g_L^2)\mathcal{G}_2 \,, \tag{3}$$

with

$$\begin{aligned} \mathcal{G}_1 \;=\; & \Big[(m_{12}^4 + \hat{s}^2)(3 + \cos 2\theta)(4\csc^2\Theta - 2) \\ & + 8m_{12}^2\,\hat{s}\,\sin^2\theta(2 + \cos 2\phi) \\ & + 8\,m_{12}\sqrt{\hat{s}}\,\left(m_{12}^2 + \hat{s}\right)\cot\Theta\,\sin 2\theta\,\cos\phi\Big] \ , \end{aligned} \tag{4}$$

$$\begin{aligned} \mathcal{G}_2 \;=\; & 16\csc\Theta\left[(m_{12}^4 + \hat{s}^2)\cos\theta\cot\Theta\right. \\ & \left. + \,m_{12}\sqrt{\hat{s}}\left(m_{12}^2 + \hat{s}\right)\,\sin\theta\cos\phi\right] \ , \end{aligned} \tag{5}$$

where $g_{L(\ell)}$ and $g_{R(r)}$ are the Z couplings to left- and right-handed quarks (leptons), m_{12} is the invariant mass of the Z (which in general can be off-shell), and $\hat{s}$ is the invariant mass of the $Z\gamma$ system. Since at a pp collider like the LHC the direction of the initial quark (as opposed to antiquark) is not known, we must sum over both possibilities. At leading order, the expression for the differential cross section with the initial quark in the opposite direction is obtained from Eq. 3- 5 by making the replacements $\Theta \to \pi - \Theta$ and $\phi \to \phi + \pi$.

In Fig. 2 we show the leading order distributions in $\cos\Theta$, ϕ, and $\cos\theta$ for a 125 GeV Higgs boson and a background process $d\bar{d} \to Z\gamma$ at $\sqrt{\hat{s}} = 125$ GeV at the parton level. These will be modified, as in the next section, after including the effects of parton distribution functions (PDF), detector acceptance, and isolation cuts. In particular, we note that $\cos\Theta$ is directly connected to the photon p_T at leading order through

$$\cos\Theta = \sqrt{1 - 4p_{\gamma T}^2\hat{s}/(\hat{s} - m_Z^2)^2} \, . \tag{6}$$

The $\cos\Theta$ distribution in Fig. 2 therefore implies that the $p_{\gamma T}$ distribution is peaked at zero for the background and $(m_h^2 - m_Z^2)/(2m_h)$ for the signal. However it also follows that once a cut on $p_{\gamma T}$ is imposed, very little additional sensitivity can be gained from the $\cos\Theta$ distribution.

Analysis and Results – We perform Monte Carlo simulations to obtain projections for the sensitivity of this channel at the LHC using various analyses. We consider Higgs masses of 120, 125, and 130 GeV. Our simulations are specific to the 8 and 14 TeV LHC. The existing

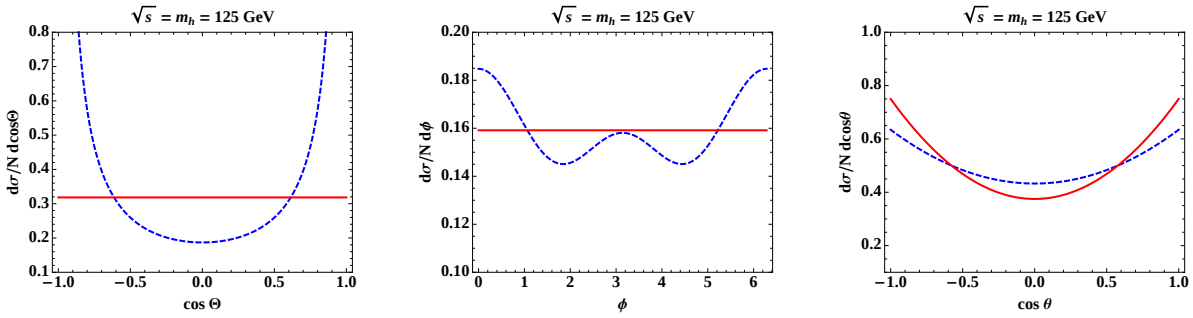

FIG. 2: *Signal (red, solid) and background (blue, dashed) distributions in* $\cos\Theta$, ϕ *and* $\cos\theta$, *with* $\sqrt{\hat{s}} = m_h = 125$ *GeV.*

7 TeV data has very little sensitivity in this channel, so we do not report those results here.

To perform these Monte Carlo studies, we generate at least 50,000 events for each signal and background process using MadGraph 5 [14]. The Higgs coupling to gluons and the $hZ\gamma$ vertex are implemented as effective dimension five operators using the HEFT model provided by MadGraph 5 and the FeynRules [15] package. For both signal and background, the processes $pp \to Z\gamma$ and $pp \to Z\gamma + 1j$ are generated, using the MLM matching scheme [16] implemented in MadGraph 5 and interfaced with Pythia 6 [17], with a matching scale of 25 GeV. We consider events with extra radiation to address one concern with the use of leading order matrix elements. The issue of using the matrix element method for events with additional radiation has been studied [18], and techniques for using next to leading order matrix elements are being developed [19].

The events generated in MadGraph are then passed to PGS 4 using the CMS parameter card [20], to model detector acceptance and smearing effects. Since the energy and momentum resolution is crucial for this analysis, we have compared the invariant mass resolution obtained from PGS 4 with the one that is obtained when smearing parton level events by hand using the CMS detector parameters [21], and found that they agree in general.

We demand that each lepton or photon have

$$|\eta| < 2.5 \quad \text{and} \quad p_T > 15 \text{ GeV}. \tag{7}$$

The smearing results in the broadening of the lineshape in the total invariant mass of the $Z\gamma$ system, $m_{\ell\ell\gamma}$, for the signal events. Therefore, before performing more detailed analyses, we perform an invariant mass cut; demanding that the invariant mass of the $Z\gamma$ system be within 5 GeV of the mean invariant mass of the $Z\gamma$ system, as measured in simulated signal events. It is worth emphasizing that since subsequent analyses will effectively reduce the range of invariant mass considered, the specific details of this initial cut does not have a strong effect on the final value of $S/\sqrt{B}$ obtained. Note that this cut also effectively removes the background coming from FSR radiation that is characterized by $m_{\ell\ell\gamma} \sim M_Z$.

To determine the expected number of signal events at the 14 TeV LHC, we obtain the inclusive Higgs production cross section from [22]. For the 8 TeV LHC, we use the values given in [23]. The branching fraction for $h \to Z\gamma$ is found using HDECAY [4], while we use the PDG value (6.73%) for the branching fraction for a Z decaying to leptons [24]. The background cross section is found by using MCFM [25, 26] with FSR photon radiation turned off.

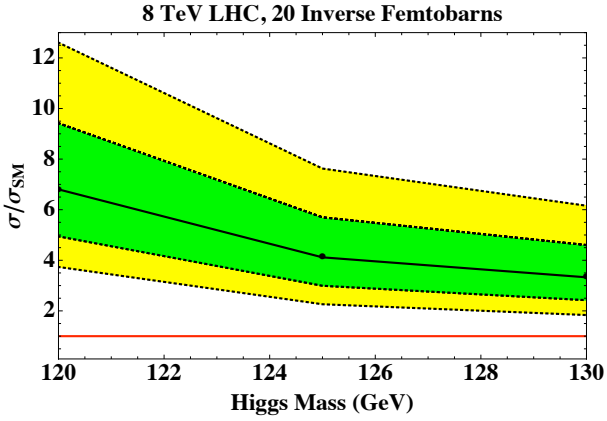

FIG. 3: *Exclusion limits at the 95% confidence level on the Higgs production rate times branching fraction to* $Z\gamma$ *at the* 8 *TeV LHC with an integrated luminosity of 20* fb^{-1}. *The green (yellow) band is the 1(2)* σ *contour. The solid red line corresponds to the SM expectation.*

We perform three analyses, two of which are multivariate. The multivariate discriminants we use are based on the matrix elements of the signal and background processes. In the context of a maximum likelihood analysis such a discriminant was used in the discovery of the single top production in [27]. For simplicity we use a cut-based approach to determining our sensitivity using these multivariate discriminants.

We construct a discriminant using the fully differential cross sections computed for the signal and background processes to quantify the relative probability of a particular event being signal-like or background-like. We then determine an optimal cut on the discriminant to maximize the value for $S/\sqrt{B}$. In one analysis, we include

PDF weights for the leading initial state for signal or background events (gg or $q\bar{q}$ respectively). In the second multivariate analysis, we do not include a weight from PDFs. Labelling the signal and background differential cross sections by $s(\mathbf{\Omega})$ and $b(\mathbf{\Omega})$, respectively, we consider the quantity

$$D(\mathbf{\Omega}) = \frac{s(\mathbf{\Omega})}{s(\mathbf{\Omega}) + b(\mathbf{\Omega})} = \left(1 + \frac{s(\mathbf{\Omega})}{b(\mathbf{\Omega})}\right)^{-1}. \qquad (8)$$

Here, $\mathbf{\Omega} = \{x_1, x_2, \hat{s}, m_{\ell\bar{\ell}}, \Theta, \theta, \phi\}$ is the complete set of kinematic observables characterizing each event. When evaluating D on a sample of pure signal events the distribution is peaked toward 1 while it is peaked toward 0 for a pure background sample. Note however, that in general neither the signal nor the background differential cross section to produce a final state with given kinematics vanishes, and thus $D(\mathbf{\Omega})$, in general, will not reach 0 or 1.

For each Higgs mass, a cut on D is determined by maximizing $S/\sqrt{B}$ of the events passing the cut. We note that a cut on $D(\mathbf{\Omega})$ is equivalent to a cut on $s(\mathbf{\Omega})/b(\mathbf{\Omega})$. Thus, the increase in sensitivity obtained using a particular cut on $D(\mathbf{\Omega})$ is independent of the normalizations of the signal and the background. While this feature motivates the use of a cut-based analysis, there is the drawback that by performing a cut-based analysis, we lose those events not passing the cut, which would not be the case if the signal and background matrix elements were used to construct the likelihood directly.

Our multivariate discriminants use the parton-level leading order differential cross section except for the Higgs propagator, as for the Higgs masses considered the Higgs width is much narrower than the experimental resolution. In principle, one can deal with this issue by using transfer functions for the lepton momenta. We take the simpler approach of weighting each event with a Gaussian invariant mass distribution that is centered at the average invariant mass for signal events. The width used in this Gaussian weighting is found by scanning (in 20 MeV increments) over potential values, from 100 MeV to 5 GeV, and selecting the value which maximizes the sensitivity of the analysis. The third analysis uses a discriminant based on the same Gaussian invariant mass weight but uses no other kinematic information about the events. While one would expect a loss of sensitivity, this approach has the advantage of being less sensitive to higher order corrections that could modify the angular distributions that enter the multivariate analyses.

We find the best values for $S/\sqrt{B}$ from the analysis in which the full differential cross sections and PDF weights are used. However the sensitivity from this analysis is only $\sim 1\%$ larger than that obtained from the invariant mass only analysis. The smallness of this increase in sensitivity is due to the fact that the relatively hard $p_{\gamma T}$ cut leaves us without much additional sensitivity to Θ, and the other angular variables are not as sensitive, especially given geometric acceptance and finite momentum resolution. We therefore quote results using the invariant mass only analysis, as they should be more robust with respect to systematic uncertainties. In particular, the $m_{\ell\ell\gamma}$ distribution is unaffected by jet radiation, so that corrections to the jet multiplicity and momentum distribution, which is only simulated to leading order in our analysis, will not reduce the sensitivity.

Higgs Mass	Signal (fb)	Backg. (fb)	$S/\sqrt{B}$ (20 fb^{-1})
120 GeV	0.38 (0.45)	32. (110)	0.30 (0.19)
125 GeV	0.61 (0.74)	30. (100)	0.50 (0.33)
130 GeV	0.66 (0.86)	23. (89.)	0.62 (0.41)

TABLE I: *The signal and background cross sections, as well as the significance after an optimal cut on the discriminant in Eq. (8) in the invariant mass only analysis at the* 8 *TeV LHC. In the parenthesis we also show the corresponding values for all events passing the* p_T *and geometric acceptance cuts and which are within an invariant mass window of* 10 *GeV centered on the Higgs mass, as described in the text.*

Higgs Mass	Signal (fb)	Backg. (fb)	$S/\sqrt{B}$ (100 fb^{-1})
120 GeV	0.83 (1.0)	36. (180)	1.2 (0.78)
125 GeV	1.3 (1.6)	37. (160)	2.0 (1.3)
130 GeV	1.7 (2.1)	40. (140)	2.7 (1.8)

TABLE II: *Same as Tab. I, for the* 14 *TeV LHC, with a luminosity of* 100 *fb*$^{-1}$.

The signal and background cross sections after the optimal cut on D from this invariant mass only analysis are listed in Table I for various Higgs masses at the 8 TeV LHC. The expected significance with 20 fb^{-1} integrated luminosity is also provided. Table II shows analogous information for the 14 TeV; here the expected significance with 100 fb^{-1} is shown.

In the absence of any signal, we have also considered the expected exclusion limit on the Higgs production rate in the gluon fusion channel using the CL$_s$ method [28] with 20 fb^{-1} of integrated luminosity for the 8 TeV LHC in Fig. 3 and for the 14 TeV LHC with 100 fb^{-1} in Fig. 4.

Conclusions – We have considered the possibility of searching for a light Higgs boson in its decays to $\ell\bar{\ell}\gamma$ final states via $Z\gamma$. This branching ratio is known precisely in the SM, and deviations from this rate are unambiguous signals of new physics that couples to the Higgs boson, or could even signal the presence of a Higgs imposter [10].

We have performed a detailed Monte Carlo study for the 8 and 14 TeV LHC. We find that branching ratios for the Higgs decay to $Z\gamma$ of several times the SM rate are probed at 8 TeV with 20 fb^{-1}, while the SM rate is probed at the 14 TeV LHC with 100 fb^{-1}. For Higgs masses of 125 GeV and above, a measurement of the Higgs branching ratio to $Z\gamma$ is in reach of the 14 TeV LHC. We hope this work inspires experimental efforts in this particular search channel.

Acknowledgments – We benefitted from discussions with B. Auerbach, S. Chekanov, A. Kobach, H. Schellman, and M. Valesco. The model file for Higgs to Zγ de-

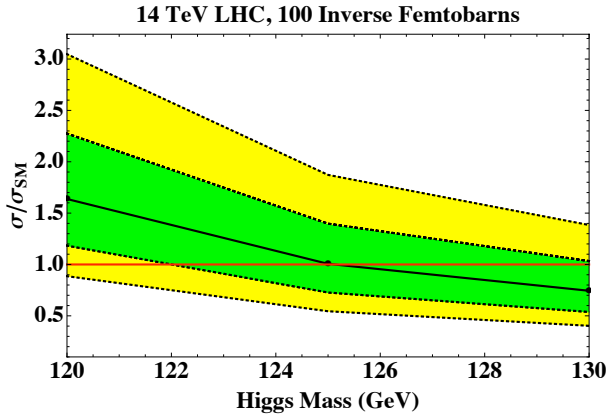

FIG. 4: *Exclusion limits at the 95% confidence level on the Higgs production rate times branching fraction to $Z\gamma$ at the 14 TeV LHC with an integrated luminosity of 100 fb^{-1}. The green (yellow) band is the 1(2) σ contour. The solid red line corresponds to the SM expectation.*

cays was prepared by R. Vega-Morales; K. Kumar aided in the construction of our figures. I.L. and P.S. acknowledge the hospitality from the CERN TH-LPCC summer institute on LHC physics, where part of this work was performed. J.S.G. acknowledges the Aspen Center for Physics and the NSF Grant #1066293 for hospitality while revising this article. This work was supported in part by the U.S. Department of Energy under contract numbers DE-AC02-06CH11357, DE-FG02-91ER40684, and DE-FG02-84ER40173.

[1] G. Aad *et al.* [ATLAS Collaboration], Phys. Lett. B **710**, 49 (2012) [arXiv:1202.1408 [hep-ex]].
[2] S. Chatrchyan *et al.* [CMS Collaboration], Phys. Lett. B **710**, 26 (2012) [arXiv:1202.1488 [hep-ex]].
[3] R. N. Cahn, M. S. Chanowitz and N. Fleishon, Phys. Lett. B **82**, 113 (1979). L. Bergstrom and G. Hulth, Nucl. Phys. B **259**, 137 (1985) [Erratum-ibid. B **276**, 744 (1986)].
[4] A. Djouadi, J. Kalinowski and M. Spira, Comput. Phys. Commun. **108**, 56 (1998). [arXiv:hep-ph/9704448].
[5] A. Freitas and P. Schwaller, JHEP **1101**, 022 (2011). [arXiv:1010.2528 [hep-ph]].
[6] T. Matsuura and J. J. van der Bij, Z. Phys. C **51**, 259 (1991); S. Y. Choi, D. J. . Miller, M. M. Muhlleitner and P. M. Zerwas, Phys. Lett. B **553**, 61 (2003); [arXiv:hep-ph/0210077]; C. P. Buszello, I. Fleck, P. Marquard and J. J. van der Bij, Eur. Phys. J. C **32**, 209 (2004); [arXiv:hep-ph/0212396]; Y. Gao, A. V. Gritsan, Z. Guo, K. Melnikov, M. Schulze and N. V. Tran, Phys. Rev. D **81**, 075022 (2010); [arXiv:1001.3396 [hep-ph]]; A. De Rujula, J. Lykken, M. Pierini, C. Rogan and M. Spiropulu, Phys. Rev. D **82**, 013003 (2010). [arXiv:1001.5300 [hep-ph]];
[7] W. Y. Keung, I. Low and J. Shu, Phys. Rev. Lett. **101**, 091802 (2008); [arXiv:0806.2864 [hep-ph]]; Q. H. Cao, C. B. Jackson, W. Y. Keung, I. Low and J. Shu, Phys. Rev. D **81**, 015010 (2010). [arXiv:0911.3398 [hep-ph]];
[8] J. S. Gainer, K. Kumar, I. Low and R. Vega-Morales, JHEP **1111**, 027 (2011) [arXiv:1108.2274 [hep-ph]].
[9] I. Low and J. Lykken, JHEP **1010**, 053 (2010). [arXiv:1005.0872 [hep-ph]].
[10] I. Low, J. Lykken and G. Shaughnessy, Phys. Rev. D **84**, 035027 (2011). [arXiv:1105.4587 [hep-ph]].
[11] Chekanov, Sergei. Private communication.
[12] Velasco, Mayda. Private communication.
[13] K. Hagiwara, R. D. Peccei, D. Zeppenfeld and K. Hikasa, Nucl. Phys. B **282**, 253 (1987); K. Hagiwara and D. Zeppenfeld, Nucl. Phys. B **274**, 1 (1986).
[14] J. Alwall, M. Herquet, F. Maltoni, O. Mattelaer and T. Stelzer, JHEP **1106**, 128 (2011). [arXiv:1106.0522 [hep-ph]].
[15] N. D. Christensen and C. Duhr, Comput. Phys. Commun. **180**, 1614 (2009) [arXiv:0806.4194 [hep-ph]].
[16] S. Hoeche, F. Krauss, N. Lavesson, L. Lonnblad, M. Mangano, A. Schalicke and S. Schumann, [arXiv:hep-ph/0602031].
[17] T. Sjostrand, S. Mrenna and P. Z. Skands, JHEP **0605**, 026 (2006) [hep-ph/0603175].
[18] J. Alwall, A. Freitas and O. Mattelaer, Phys. Rev. D **83**, 074010 (2011) [arXiv:1010.2263 [hep-ph]].
[19] J. M. Campbell, W. T. Giele and C. Williams, [arXiv:1204.4424 [hep-ph]].
[20] `http://physics.ucdavis.edu/~conway/research/software/pgs/pgs4-general.htm`
[21] G. L. Bayatian *et al.* [CMS Collaboration], CMS-TDR-008-1, 2006.
[22] S. Dittmaier *et al.*,[arXiv:1101.0593 [hep-ph]].
[23] C. Anastasiou, S. Buehler, F. Herzog and A. Lazopoulos, [arXiv:1202.3638 [hep-ph]].
[24] K. Nakamura *et al.*,J. Phys. GG **37**, 075021 (2010).
[25] J. M. Campbell and R. K. Ellis, Nucl. Phys. Proc. Suppl. **205-206**, 10 (2010). [arXiv:1007.3492 [hep-ph]].
[26] J. M. Campbell, R. K. Ellis and C. Williams, JHEP **1107**, 018 (2011) [arXiv:1105.0020 [hep-ph]].
[27] V. M. Abazov *et al.* [D0 Collaboration], Phys. Rev. D **78**, 012005 (2008). [arXiv:0803.0739 [hep-ex]].
[28] A. L. Read, In *Geneva 2000, Confidence limits* 81-101.